

Hydrophobic Membranes of Tetrafluoroethylene and 2,2,4 Trifluoro 5 Trifluoromethoxy 1,3 Dioxole

A. Gordano, G. Clarizia, E. Tocci¹, and E. Drioli¹

CNR-IRMERC c/o Department of Chemical and Material Engineering, University of Calabria,
V. P. Bucci - Arcavacata of Rende (CS) I - 87030

¹Department of Chemical and Material Engineering, University of Calabria,
V. P. Bucci - Arcavacata of Rende (CS) I - 87030

(Received August 7, 1999, Accepted October 8, 1999)

Abstract: Symmetric, asymmetric and composite perfluoropolymer membranes, made with HYFLON® AD, have been prepared and evaluated. Porous and non porous symmetric membranes have been prepared by solvent evaporation with various processing conditions. Non-contact atomic force microscopy (AFM) was used to investigate the membrane morphology in air. Analysis of the images gave quantitative information on the surface pore structure, in particular on the pore size distribution. Possible useful uses of porous membranes are envisaged in the field of gas-liquid separations, such as membrane contactors (MCs). Molecular Dynamics (MD) simulations structure of HYFLON® AD 60X copolymer, supporting these results, are also reported. Amorphous perfluoropolymer membranes appears to be ideal, other than in MCs, when separation processes have to be performed in hostile environments, i.e. high temperatures and aggressive non-aqueous media, such as chemicals and solvents. In these cases HYFLON® AD membranes can exploit the outstanding resistance of perfluoropolymers.

1. Introduction

Fluoropolymers continue attracting increasing attention for a large number of high-demanding applications and, perhaps, they will do so even more in next future. Actually these materials enjoy a remarkable combination of properties unmatched by any other class of polymers. Perfluoropolymers, a specific type of these materials, represent the ultimate resistance to hostile chemical environments and high service temperature, attributed to the presence of fluorine in the polymer backbone. Copolymers of Tetrafluoroethylene (TFE) and 2,2,4 Trifluoro-5 Trifluoromethoxy-1,3 Dioxole (TTD), are amorphous perfluoropolymers commercially known as HYFLON® AD.

These amorphous perfluoropolymers are similar

to other amorphous polymers in optical clarity and mechanical properties, including strength, but also resemble fluoropolymers in their performance over a wide range of temperatures, outstanding electrical properties and chemical resistance.

Copolymers of TFE and TTD represent an important class of advanced materials exhibiting one of the highest thermal and thermal-oxidative stability, coupled with excellent chemical resistance and superior electrical insulating ability.

TFE-TTD copolymers are highly transparent to light from deep UV to near infrared, so they find applications in optic and electronic industries, such as plastic optical fibers, antireflective coating and protective pellicles in semiconductor manufacture.

Perfluoropolymers represent the ultimate resistance to hostile chemical environments and high

service temperature, due to the high bond energy of C-F (485 kJ/mol) and C-C (360 kJ/mol) bonds of fluorocarbons. In many applications they offer the highest protection of any polymer available today to a huge variety of chemicals, such as acids and alkalis, fuels and oils, low molecular weight esters, ethers and ketones, aliphatic and aromatics amines, strong oxidizing substances.

Copolymers of TFE and TTD are amorphous perfluoropolymers with glass transition temperature higher than room temperature. They show a thermal decomposition temperature exceeding 400°C. An important peculiarity of these amorphous perfluoropolymers is their high solubility in fluorinated solvents, with low viscosity, that leads to the possibility to dissolve them in certain perfluorinated solvents for the production of highly uniform self-supported and composite membranes with desired membrane thickness.

In the present work the preparation and evaluation of symmetric, asymmetric and composite membranes made with HYFLON® AD are presented. Morphological properties of these membranes were investigated by following various techniques and separation properties to water and single gases were also considered. The molecular modeling (MD) technique due to recent progress in developing of force fields and high-speed computing facilities MD simulations has begun to be focused on the study of diffusional processes of glassy amorphous polymers. MD simulation were performed to explore at atomistic level the polymeric structure of HYFLON® AD 60X copolymer and to understand the relations between structure/transport properties.

2. Materials and Methods

HYFLON® AD 60X and HYFLON® AD 80X used in this work are characterized by a T_g of 110 and 135°C, respectively. They differ in the TTD contents that are, respectively, about 60 and 85 %mole.

2.1. Membrane Preparation

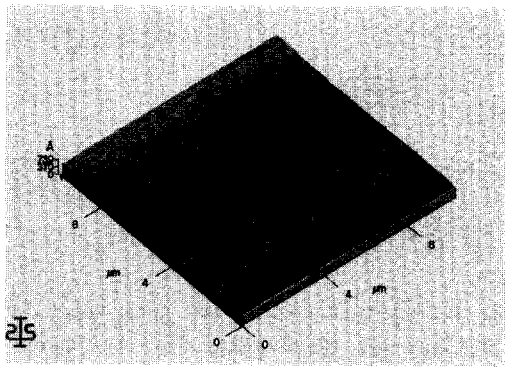
Flat sheet membranes from HYFLON® AD 60X were prepared by following evaporation method [1],

using both Galden HT 55 and Galden HT 110 as solvents for the polymers. The polymeric solution (10% wt/wt) was obtained dissolving the polymer by magnetically stirring for one day or more to allow complete solution at room temperature. To cast the polymeric solution on glass plate a Braive Instruments knife with initial thickness of 250 μm was used. Three different porous membranes, named respectively A1, A2 and A3, were prepared at different temperature, 13, 24 and 36°C; in this case the solvent was Galden HT 55. Flat sheet asymmetric membranes were prepared following the dry-wet phase inversion method, with 10% wt/wt polymeric solutions. The solvent was Galden HT 55, the non-solvent *n*-pentane [2]. A Braive Instruments knife with initial thickness of 250 μm was also used in this case to cast the polymeric film on glass plates. Two different membranes were prepared at two different coagulation bath temperatures, 12 and 20°C. Flat sheet composite membranes of 1 micron thickness film on a PVDF support were prepared, using both HYFLON® AD 60X and HYFLON® AD 80X, by the spin coating process.

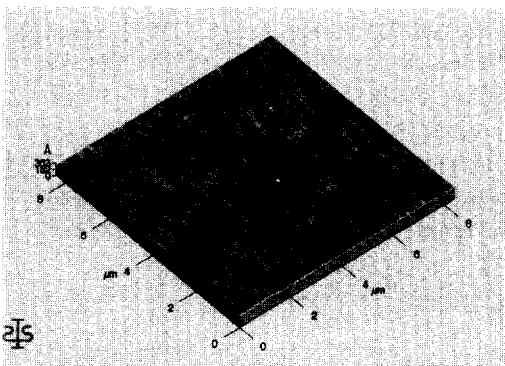
2.2. Instruments

Contact angles to water and hexadecane were measured by a Contact Angle Meter CAM 100 of KSV Instruments Ltd. The AFM [3] used in the present study was an Autoprobe (CP-100), a commercial device from Park Scientific Instruments (USA).

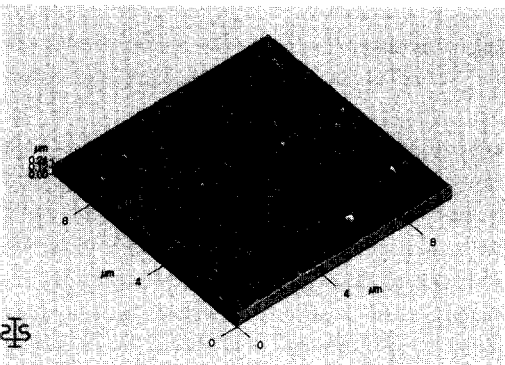
High magnification images of membrane surfaces can be obtained with the use of microfabricated cantilevers [4]. In the present work, Ultralevers (Park Scientific Instruments) were used. A stiff silicon cantilever with a high aspect ratio tip with typical curvature radius of 10 nm was vibrated near its resonance frequency (typically 100-400 kHz) with an amplitude of a few nanometers. Changes in the cantilever resonance were detected as the tip was scanned above the membrane surface. Vertical motion of the tip, due to interatomic forces, was detected by sensing, with a two segment photodiode, the deflection of a laser beam reflected off the back of the cantilever. Measure-



(a)



(b)



(c)

Fig. 3(a-c). AFM micrographs of A1, A2 and A3 membranes over a scanned area of $10 \times 10 \mu\text{m} \times \mu\text{m}$.

The AFM software allows quantitative determination of the diameter of pores by the use of the image in conjunction with digitally stored line profiles [6]. The simultaneous use of images and

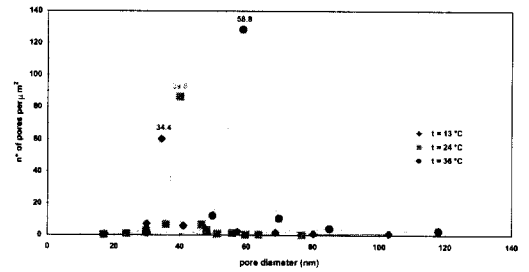


Fig. 4. Pore size distribution for A1, A2 and A3 membranes.

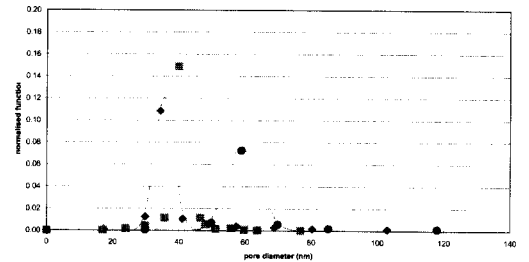


Fig. 5. Symmetric and asymmetric distribution functions for A1, A2 and A3 membranes.

profiles greatly facilitates identification of the entrance of individual pores. Pore diameters were determined in this way for about 1000 pores for the A1 membrane, 2000 for the A2 membrane and 2500 pores for A3 membrane. Pore diameters determined for the membranes A1, A2 and A3, respectively, results 34.4, 39.8 and 58.8 nm. The resulting pore size distributions are shown in Fig. 4.

The membrane morphology plays an important role in many applications of the membranes and, in particular, pore size distribution [7]. The effect of the distribution of pore diameters depends on the shape of the distribution itself. Symmetric and asymmetric distribution functions were considered. Fig. 5 reports both of the function over the experimental data for the three membranes. The symmetric function is represented by the continuous line, while the asymmetric by the sketched one. It's clear from the figure, that in both of the function the bigger and the smaller pores have a little importance, compared to the value at the top of distribution, that leads to a good agreement with the experimental data. The trend of the function is

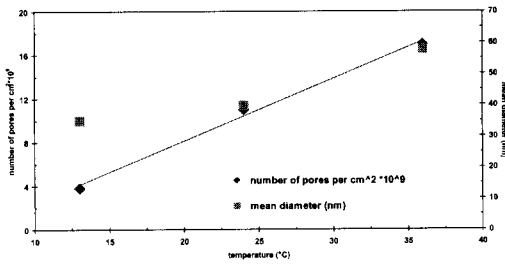


Fig. 6. Numbers of pores and mean pore diameter versus evaporation temperature.

similar for symmetric and asymmetric one, even if a little difference in the value of the peak is registered. These data show that the membranes have a narrow pore size distribution. The equations of the symmetric and asymmetric normalised distribution functions are reported below.

$$f(x)_{\text{symm.}} = \frac{1}{A_0^{\text{symm.}}} \exp \left[-\frac{(x - \bar{d})^2}{\sigma_{\text{symm.}}^2} \right]$$

$$f(x)_{\text{asymm.}} = \frac{1}{A_0^{\text{symm.}}} \exp \left[-\frac{\log(x/\bar{d})}{\sigma_{\text{symm.}}} \right]$$

Where A_0 represents the area, x is the pore diameter and mean diameter (\bar{d}) and σ^2 are so defined:

$$\bar{d} = \int_0^\infty xf(x)dx$$

$$\sigma^2 = \int_0^\infty (x - \bar{d})^2 f(x)dx$$

The Fig. 6 reports the number of pores and the pore diameters versus evaporation temperature. It's clear that the number of pores per cm² increases linearly when evaporation temperature increase. The pore diameter increases also, but non linearly; it may depend on the evaporation time.

Superficial porosity of these membranes was also determined by using the same data. Fig. 7 shows the values of superficial porosity and mean superficial porosity for the membranes analyzed by using AFM software. The percentage porosity was calculated by dividing the total pores area by the total analyzed membrane surface. In the first case,

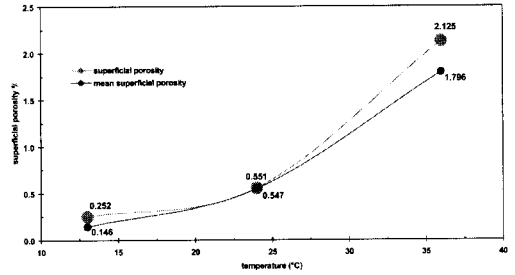


Fig. 7. Superficial porosity and mean superficial porosity versus evaporation temperature.

the real area of each pore was considered, while mean superficial porosity was calculated by considering all pores with the same diameter, that is the one on the peak of the distribution function.

Asymmetric membranes were also analyzed by using AFM technique, but in this case, no pores were present over the scanned area, according to the dense top layer of asymmetric membranes.

3.3. Gas Permeability

Symmetric porous membranes with pore size between 30 and 80 nm have shown no permeation to water at pressures as high as 10 bars. However high permeation to gases, such as O₂, N₂ and CO₂ were observed. No selectivity to single gases were measured, as expected, considering the porous structure of the membranes. In consideration of the above properties, possible useful uses in the field of gas-liquid separations are envisaged for these membranes. Particularly promising applications can be found in the field of membrane contactors, i.e. equipment in which membranes are used to improve mass transfer coefficients in respect to traditional extraction and absorption processes.

The characterization of asymmetric membrane samples in steady state conditions gave selectivity values for O₂/N₂ and CO₂/N₂ around 3 and 8 respectively in pressure range of 5-7.5 kg/cm². Table 1 gives mean permeability values to N₂, CO₂ and O₂. Selectivity values for two different coagulation bath temperatures are reported in Tables 2 and 3. Permeability and selectivity found on asymmetric membranes are in good agreement

with values found on composite membranes. Permeability properties to N_2 , O_2 , CH_4 , H_2 and CO_2 of composite membranes are reported in Table 4.

3.4. Structure-permeation Correlation in Amorphous Perfluoropolymers

Gas permeation is often attributed to the presence of voids on the molecular scale and to their size distribution. The voids volume fraction (Φ_v) of TTD-TFE amorphous perfluoropolymers were

Table 1. Mean Permeance at @T for AD 60X Asymmetric Samples Coagulated at 12°C

Δp , kg/cm ²	P(N ₂), GPU	P(CO ₂), GPU	P(O ₂), GPU
1.		15.3	6
5	1.7	14	5.3
7.5	1.7	14.7	5.3
10	1.8	15.3	

Table 2. Selectivities at @T for O₂/N₂ and CO₂/N₂ through AD 60X Asymmetric Membranes Coagulated at 12°C

Δp , kg/cm ²	O ₂ /N ₂	CO ₂ /N ₂
5	3.1	8.2
7.5	3.1	8.5
10		8.5

Table 3. Selectivities at @T for O₂/N₂ and CO₂/N₂ through AD 60X Asymmetric Membranes Coagulated at 20°C

Δp , kg/cm ²	O ₂ /N ₂	CO ₂ /N ₂
5	3.2	7.9
7.5	3.2	7.9
10		7.9

Table 4. Permeability Data (expressed in Barrer) of Amorphous Perfluoropolymers

Type of polymer	Tg (°C)	P(O ₂)	P(N ₂)	P(CH ₄)	P(H ₂)	P(CO ₂)
Hyflon AD 40X	91	26	8.1			64
Hyflon AD 60X	110	51.4	16.5	8.01	202	124
Hyflon AD 80X	134	194	76.8	48.9	563	473
TEFLON AF 1600	160	340				
TEFLON AF 2400	240	490	490	340	2200	2800

estimated from the difference between the experimental polymer density and a theoretical density obtained from the Van der Waals molar volume through a general constant. Van der Waals molar volume were estimated by the group contribution method. Table 6 shows the oxygen permeation and the estimated Φ_v for two TTD-TFE copolymers, i.e. HYFLON® AD 60X and HYFLON® AD 80X, having different monomer compositions.

Considering the chemical structure of amorphous perfluoropolymers, the low values of the measured density in comparison to the theoretical one, can be ascribed, at least qualitatively, to the different chain packing due to the low chain mobility and steric hindrance given by the large dioxole groups [8]. In other words, the high chain stiffness leads to difficulties in the close packing of chain segments and then to "nanovoids". The amount of free volume and how free volume elements are interconnected in the formation of nanovoids are mainly controlled by the chain stiffness. The polymer containing the higher amount of the TTD dioxole monomer shows a much higher gas permeability, although the estimated Φ_v increases only slightly.

A better correlation was found between permeation and another quantity mainly related to chain stiffness. This is the glass transition temperature (Tg). In the case of perfluoropolymers, Tg is mainly related to chain stiffness since the contribution of intermolecular interactions is very low due to the presence of fluorine atoms in the polymer backbone. We believe that in the special case of amorphous perfluoropolymers, this good correlation is obtained because both these quantities are related to chain stiffness. Permeation v.s. Tg referred to different molecules, such as oxygen, nitrogen, hydrogen, methane and carbon dioxide for

Table 5. Oxygen Permeation Rate as Function of Different Copolymer Composition and related Void Volume Fraction

Polymer	TFE % mol	TTD % mol	PDD % mol	Φ_v	PO ₂ , Barrer
Hyflon AD 40X	60	40	-		26
Hyflon AD 60X	40	60	-	9.4	51.4
Hyflon AD 80X	15	85	-	9.5	190
TEFLON AF 1600	35	-	65	14.8	340
TEFLON AF 2400	10	-	90	17.7	990

different amorphous perfluoropolymers, have been reported elsewhere. The surprisingly linear relationship observed between permeation and Tg is under investigation.

3.5. Molecular Dynamics

The MD simulations were made with a Silicon Graphics ORIGIN 2000 and with a CRAY super-computer at the CINECA computing centre. Molecular dynamics simulations were carried out for a single chain models of tetrafluoroethylene (TFE) and 2,2,4 trifluoromethoxy 1,3dioxole (TTD). The distribution of repeat units was done in statistical way, with conditional probabilities. The simulated chain of random copolymer HYFLON® AD 60 X follow the experimental concentrations of TFE (60%) and TTD (40%) monomers. The model construction was performed with Polymerizer module of MSI [9].

The chain is grown with the Theodorou and Suter approach [10] with reproducing the conformational statistics of the backbone dihedral angles present in a real amorphous polymer and the measured density. In this study we employ *pcff* force field which is an extension of the Consistent Force field *cff91* [11] which is intended for polymer and organic material applications [12-14].

The force field describes the potential energy function for all different types of interactions involved in the diffusion of small penetrant molecules in a polymer matrix (bond stretching, bond angle bending, bond torsions, nonbonded *van der Waals* interactions, etc.). The potential terms of the *pcff* force field are described by a quartic expression for bond stretch

$$E_b = \sum_{ij} [K_2(b - b_0)^2 + K_3(b - b_0)^3 + K_4(b - b_0)^4] \quad (1)$$

where b_0 is the equilibrium bond length, b is the bond length in the simulated polymer and K_2 , K_3 and K_4 are force constants and for bond bend

$$E_\theta = \sum_{ij} [H_2(\theta - \theta_0)^2 + H_3(\theta - \theta_0)^3 + H_4(\theta - \theta_0)^4] \quad (2)$$

where θ_0 is the equilibrium bond angle measured experimentally, θ is the bond angle of the simulated polymer and H_2 , H_3 and H_4 are the corresponding force constants.

The potential form for torsional term is :

$$E_\phi = [V_1(1 - \cos \phi) + V_2(1 - \cos 2\phi) + V_3(1 - \cos 3\phi)] \quad (3)$$

where V_1 , V_2 and V_3 are force constants and ϕ is the dihedral angle.

The non-bonded interactions, "soft" Lennard-Jones 6-9 potential and electrostatic terms were estimated as follow:

$$E(r) = \sum_{i,j} \epsilon_{ij} \left[2 \left(\frac{r_{ij}^9}{r_{ij}^6} \right) - 3 \left(\frac{r_{ij}^6}{r_{ij}^3} \right) \right] + \sum_{ij} \frac{q_i q_j}{r_{ij}} \quad (4)$$

where ϵ_{ij} , q_i , q_j are the dielectric constant and the electrical charges respectively.

Periodic boundary conditions were imposed on a cubic unit cell of 15 Å in order to eliminate surface effects. A completely amorphous polymer box of about 3.5 nanometers (nm) was considered. In order to reduce the effect of terminal chain ends, one polymer chain of about 3000 atoms was considered.

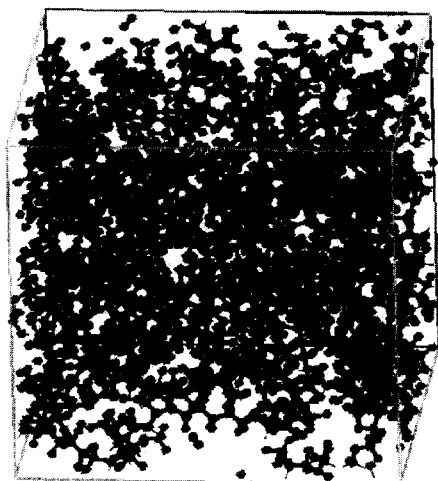
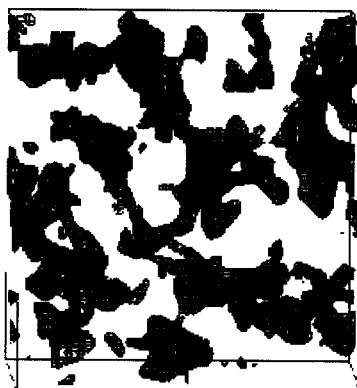


Fig. 8. Polymer model of HYFLON® AD 60 X.

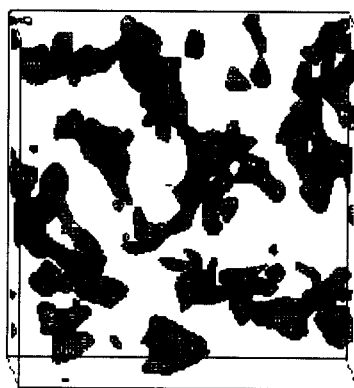
Fig. 8 shows a well refined system with a homogeneous distribution of the polymer chain segment at the experimental density. TTD-TFE perfluoro copolymer membranes show a high void volume fraction.

The amount of free volume and its distribution (that control the gas molecule diffusion) is visualized in Fig. 9. Here oxygen and nitrogen molecules were used as probe molecule. Also in this case the presence of large holes can be observed. The analysis of such a map give indication that the amount of free volume is relatively large (in comparison with other glassy polymers like PEEK-WC [15]) and that the holes are interconnected by channels of the dimension of some Angstrom with each others. In particular it has been observed that the voids the oxygen molecules can visit are larger than the free region for nitrogen. This is understandable considering that nitrogen has the a larger kinetic diameter than oxygen and this result can be related to the different permeant behaviour of two gases.

From the above results, Molecular Dynamics is confirmed to be useful tool to study permeation behaviours in polymer systems. The low density of amorphous perfluoropolymers, the formation of nano-size holes and the permeation-glass transition temperature correlation, are in good agreement with Molecular Dynamic studies.



(a)



(b)

Fig. 9. Representation of the free volume distribution using oxygen (a) and nitrogen (b) as probe molecule.

4. Conclusions

Symmetric and asymmetric membranes, made with HYFLON® AD, have been prepared and evaluated. Porous and non porous membranes have been obtained by traditional evaporation and dry-wet phase inversion processes.

All membranes showed very high contact angle to water and high contact angle to hexadecane, demonstrating a high hydrophobic character and low fouling tendency.

Porous membranes with pore size between 30 and 80 nm have shown no permeation to water at pressures as high as 10 bars. However high permeation to gases, such as O₂, N₂ and CO₂, and no

selectivity were observed. Considering the porous structure of the membrane, this behaviour was expected.

In consideration of the above properties, possible useful uses in the field of gas-liquid separations are envisaged for these membranes. A particularly promising application is in the field of membrane contactors and equipments in which membranes are used to improve mass transfer coefficients in respect to traditional extraction and absorption processes.

Gas permeation properties have been evaluated for asymmetric membranes and composite symmetric ones. Experimental data, compared with literature data obtained with membranes made with different amorphous perfluoropolymer systems, are reported. Results are discussed in terms of polymer chain structure, which affects the presence of voids at molecular scale and their size distribution. Molecular Dynamics studies supporting these results, are also reported.

Atomic force microscopy is an effective means of investigations the surface structure and morphology of the membranes. Image analysis can provide detailed information on the surface pore structure and pore distribution. The results reveal that the membranes show a narrow size distribution. Normalised distribution functions were also determined.

Separation processes performed in hostile environments, i.e. high temperatures aggressive non-aqueous media, such as chemicals and solvents, might be an interesting area in the use of these membranes realised with a perfluorinated polymer.

Acknowledgments

The authors thanks Dr. Maria De Santo and Eng. Fortunato Lagan for their support of this research.

References

1. K. Kimmerle and H. Strathmann, *Desalination*, **79**, 283-302 (1990).
2. Patent application required.
3. A. K. Fritzsche, A. R. Arevalo, M. D. Moore and C. O'Hara, *J. Membrane Sci.*, **81**, 109-120 (1993).
4. T. R. Albrecht and C. F. Quate, *J. Vac. Sci. Technol. A*, **6**, 271-275 (1988).
5. E. Drioli et al., *Gas Sep. Purif.*, **5**, 252-258 (1991).
6. W. R. Bowen and N. J. Hall, *Biotechnol. Bioeng.*, **46**, 28-35 (1995).
7. W. R. Bowen, N. Hilal, R. W. Lovitt and P. M. Williams, *J. Membrane Sci.*, **110**, 233-238 (1996).
8. B. Freeman and I. Pinnau, *TRIP*, **5**, 167 (1997).
9. Polymer User Guide, Version 4.0.0P, Molecular Simulation, San Diego, 1997.
10. D. Theodorou, U. Suter, *Macromolecules*, **19**, 139 (1986).
11. J. A. Marple, M. -J. Hiwang, T. P. Stochfisch, U. Dinur, M. Waldman, C. S. Ewig, A. T. Hagler, *J. Comp. Chem.*, **15**, 162 (1994).
12. J. A. Marple, M.-J. Hiwang, T. P. Stochfisch, U. Dinur, M. Waldman, C. S. Ewig, A. T. Hagler, *J. Comp. Chem.*, **15**, 162 (1994).
13. H. Sun, *J. Comp. Chem.*, **15**, 752 (1994).
14. H. Sun, *Macromolecules*, **28**, 701 (1995).
15. E. Tocci, D. Hofmann, D. Paul, N. Russo, E. Drioli, submitted to *Polymer*.